

Determination of $\Lambda_{\overline{MS}}$ from quenched and $N_f = 2$ dynamical QCD

S. Booth^a, M. Göckeler^b, R. Horsley^c, A.C. Irving^d, B. Joo^{e 1},
S. Pickles^{e 2}, D. Pleiter^c, P.E.L. Rakow^b, G. Schierholz^{c,f},
Z. Sroczynski^{e 3}, H. Stüben^g

– QCDSF–UKQCD *Collaboration* –

^a*Edinburgh Parallel Computing Center EPCC,
University of Edinburgh, Edinburgh EH9 3JZ, UK*

^b*Institut für Theoretische Physik, Universität Regensburg,
D-93040 Regensburg, Germany*

^c*John von Neumann-Institut für Computing NIC,
Deutsches Elektronen-Synchrotron DESY, D-15735 Zeuthen, Germany*

^d*Theoretical Physics Division, Department of Mathematical Sciences,
University of Liverpool, Liverpool L69 3BX, UK*

^e*Department of Physics and Astronomy,
University of Edinburgh, Edinburgh EH9 3JZ, UK*

^f*Deutsches Elektronen-Synchrotron DESY, D-22603 Hamburg, Germany*

^g*Konrad-Zuse-Zentrum für Informationstechnik Berlin, D-14195 Berlin, Germany*

Abstract

The scale parameter $\Lambda_{\overline{MS}}$ is computed on the lattice in the quenched approximation and for $N_f = 2$ flavors of light dynamical quarks. The dynamical calculation is done with non-perturbatively $O(a)$ improved Wilson fermions. In the continuum limit we obtain $\Lambda_{\overline{MS}}^{N_f=0} = 243(1)(10)$ MeV and $\Lambda_{\overline{MS}}^{N_f=2} = 217(16)(11)$ MeV, respectively.

Key words: QCD, Lattice, Strong coupling constant, Λ parameter

PACS: 11.15.Ha, 12.38.-t, 12.38.Bx, 12.38.Gc

¹ Present address: Department of Physics, Columbia University, New York, NY 10027, USA

² Present address: Computer Services for Academic Research CSAR, University of Manchester, Manchester M13 9PL, UK

³ Present address: Fachbereich Physik, Universität Wuppertal, D-42097 Wuppertal, Germany

1 Introduction

The Λ parameter sets the scale in QCD. In the chiral limit it is the only parameter of the theory, and hence it is a quantity of fundamental interest. It is defined by the running of the strong coupling constant α_s [1] at high energies where non-perturbative effects are supposed to become small. Lattice gauge theory provides a means of determining α_s directly from low-energy quantities. In this letter we shall compute Λ on the lattice in the quenched approximation as well as for $N_f = 2$ species of degenerate dynamical quarks.

Previous lattice calculations have employed a variety of methods to compute the strong coupling constant, in quenched and unquenched simulations. For reviews see [2,3]. The scale parameter Λ has been extracted from the heavy-quark potential [4–6], the quark-gluon vertex [7], the three-gluon vertex [8,9], from the spectrum of heavy quarkonia [10–14], and by means of finite-size-scaling methods [15].

We determine Λ from the average plaquette and the force parameter r_0 [16]. Both quantities are widely computed in lattice simulations. In the quenched case we have many data points over a wide range of couplings at our disposal already, and in the dynamical case we expect to accumulate more points in the near future. At present r_0 is the best known lattice quantity, at least in full QCD. It can easily be replaced with more physical scale parameters like hadron masses or f_π when the respective data become more accurate.

2 Method

The calculations are done with the standard gauge field action

$$S_G = \beta \sum_x \text{Re} \frac{1}{3} \text{Tr} U_\square(x), \quad (1)$$

and, in the dynamical case, with non-perturbatively $O(a)$ improved Wilson fermions [17]

$$S_F = S_F^{(0)} - \frac{i}{2} \kappa_{\text{sea}} g c_{SW} a a^4 \sum_x \bar{\psi}(x) \sigma_{\mu\nu} F_{\mu\nu} \psi(x), \quad (2)$$

where $S_F^{(0)}$ is the original Wilson action and $\beta = 6/g^2$. If the improvement coefficient c_{SW} is appropriately chosen, this action removes all $O(a)$ errors from on-shell quantities. A non-perturbative evaluation of this function leads to the parameterization [18]

$$c_{SW} = \frac{1 - 0.454g^2 - 0.175g^4 - 0.012g^6 + 0.045g^8}{1 - 0.720g^2} \quad (3)$$

for $N_f = 2$ flavors, which is valid for $\beta \geq 5.2$.

The running of the coupling is described by the β function defined by

$$\mu \frac{\partial g_{\mathcal{S}}(\mu)}{\partial \mu} = \beta^{\mathcal{S}}(g_{\mathcal{S}}(\mu)), \quad (4)$$

where \mathcal{S} is any mass independent renormalization scheme. The perturbative expansion of the β function reads

$$\beta^{\mathcal{S}}(g_{\mathcal{S}}) = -g_{\mathcal{S}}^3 \left(b_0 + b_1 g_{\mathcal{S}}^2 + b_2^{\mathcal{S}} g_{\mathcal{S}}^4 + b_3^{\mathcal{S}} g_{\mathcal{S}}^6 + \dots \right). \quad (5)$$

The first two coefficients are universal,

$$\begin{aligned} b_0 &= \frac{1}{(4\pi)^2} \left(11 - \frac{2}{3} N_f \right), \\ b_1 &= \frac{1}{(4\pi)^4} \left(102 - \frac{38}{3} N_f \right), \end{aligned} \quad (6)$$

while the others are scheme dependent. The renormalization group equation (4) can be exactly solved:

$$\frac{\mu}{\Lambda_{\mathcal{S}}} = \left(b_0 g_{\mathcal{S}}^2 \right)^{\frac{b_1}{2b_0}} \exp \left(\frac{1}{2b_0 g_{\mathcal{S}}^2} + \int_0^{g_{\mathcal{S}}} d\xi \left(\frac{1}{\beta^{\mathcal{S}}(\xi)} + \frac{1}{b_0 \xi^3} - \frac{b_1}{b_0^2 \xi} \right) \right), \quad (7)$$

where the scale parameter Λ appears as the integration constant. In the \overline{MS} scheme the β function is known to four loops [19]:

$$\begin{aligned} b_2^{\overline{MS}} &= \frac{1}{(4\pi)^6} \left(\frac{2857}{2} - N_f \frac{5033}{18} + N_f^2 \frac{325}{54} \right), \\ b_3^{\overline{MS}} &= \frac{1}{(4\pi)^8} \left(\frac{149753}{6} + 3564 \zeta_3 - N_f \left(\frac{1078361}{162} + \frac{6508}{27} \zeta_3 \right) \right. \\ &\quad \left. + N_f^2 \left(\frac{50065}{162} + \frac{6472}{81} \zeta_3 \right) + N_f^3 \frac{1093}{729} \right), \end{aligned} \quad (8)$$

where $\zeta_3 = 1.20206\dots$ is Riemann's zeta function.

In this paper we are concerned with three different schemes. In the continuum we use the \overline{MS} scheme. On the lattice we consider the bare coupling $g(a)$ and the boosted coupling $g_{\square}(a)$. The latter is given by

$$g_{\square}^2(a) = \frac{g^2(a)}{P}, \quad (9)$$

where $P = (1/3) \langle \text{Tr} U_{\square} \rangle \equiv u_0^4$ is the average plaquette value. The widespread opinion is that the perturbative expansion in g_{\square} converges more rapidly than the expansion in the bare coupling [20]. Indeed, a comparison between the expansion coefficients in the two cases for the quenched plaquette shown in Fig. 1 supports this belief, as even for low orders the new series has oscillating

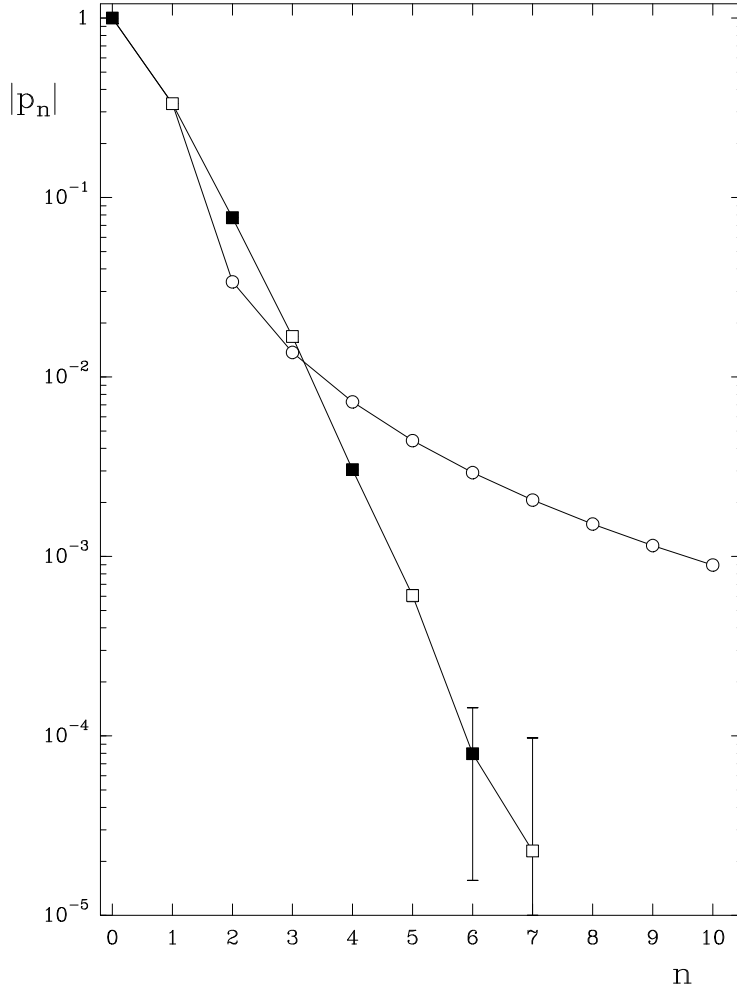


Fig. 1. The expansion coefficients for the quenched plaquette, $1 - P = \sum_{n=1}^{\infty} p_n x^n$, for $x = g^2$ (\circ) and $x = g_{\square}^2$ (\square and \blacksquare), respectively. Open (solid) symbols refer to positive (negative) numbers. The bare expansion coefficients (\circ) are taken from [21]. Note that the boosted coefficients are not only much smaller and rapidly decreasing, but also alternating in sign.

coefficients. The conversion from the bare coupling to the \overline{MS} scheme has the form

$$\frac{1}{g_{\overline{MS}}^2(\mu)} = \frac{1}{g^2(a)} + 2b_0 \ln a\mu - t_1 + (2b_1 \ln a\mu - t_2) g^2(a) + O(g^4 \ln^2 a\mu). \quad (10)$$

Writing

$$\frac{1}{g_{\square}^2} = \frac{1}{g^2} - p_1 - p_2 g^2 - p_3 g^4 - \dots, \quad (11)$$

we obtain the relation between the boosted coupling and the \overline{MS} coupling

$$\frac{1}{g_{\overline{MS}}^2(\mu)} = \frac{1}{g_{\square}^2(a)} + 2b_0 \ln a\mu - t_1 + p_1 + (2b_1 \ln a\mu - t_2 + p_2) g_{\square}^2(a) + O(g^4 \ln^2 a\mu). \quad (12)$$

By differentiating eq. (12) we can find the β function coefficient, b_2^{\square} , for the boosted coupling

$$b_2^{\square} = b_2^{\overline{MS}} + b_0(p_2 - t_2) - b_1(p_1 - t_1). \quad (13)$$

The one-loop coefficients p_1 and t_1 are given by

$$p_1 = \frac{1}{3}, \quad (14)$$

$$t_1 = 0.4682013 - N_f \left(0.0066960 - 0.0050467 c_{SW} + 0.0298435 c_{SW}^2 + am(-0.0272837 + 0.0223503 c_{SW} - 0.0070667 c_{SW}^2) \right), \quad (15)$$

where m is the quark mass. The quenched coefficients are taken from [22], whereas the fermionic contribution, including the improvement term proportional to am , is computed in the Appendix. The pure Wilson ($c_{SW} = 0$) result agrees with [23], and the $m = 0$ result agrees with the number quoted in [24]. The $m = 0$ two-loop coefficients p_2 and t_2 are given by

$$p_2 = 0.0339110 - N_f \frac{8}{3} (0.0006929 - 0.0000202 c_{SW} + 0.0005962 c_{SW}^2), \quad (16)$$

$$t_2 = 0.0556675 - N_f (0.002600 + 0.000155 c_{SW} - 0.012834 c_{SW}^2 - 0.000474 c_{SW}^3 - 0.000104 c_{SW}^4). \quad (17)$$

The two-loop am term is not known. The quenched coefficients can be found in [22], whereas the fermionic contribution to p_2 is given in [25], and t_2 has been computed in [26].

Combining these terms gives

$$\frac{1}{g_{\overline{MS}}^2(\mu)} = \frac{1}{g_{\square}^2(a)} + 2b_0 \ln a\mu - t_1^{\square} + (2b_1 \ln a\mu - t_2^{\square}) g_{\square}^2(a) + \dots \quad (18)$$

with

$$t_1^{\square} = 0.1348680 - N_f \left(0.0066960 - 0.0050467 c_{SW} + 0.0298435 c_{SW}^2 + am(-0.0272837 + 0.0223503 c_{SW} - 0.0070667 c_{SW}^2) \right), \quad (19)$$

$$t_2^{\square} = 0.0217565 - N_f (0.000753 + 0.000209 c_{SW} - 0.014424 c_{SW}^2 - 0.000474 c_{SW}^3 - 0.000104 c_{SW}^4). \quad (20)$$

Note that $t_1^\square \ll t_1$, so that the series converting g_\square to $g_{\overline{MS}}$, eq. (18), is better behaved than the original series converting bare g to $g_{\overline{MS}}$, eq. (10). We can improve the convergence of the series further by re-expressing it in terms of the tadpole improved coefficients [20]

$$\begin{aligned}\tilde{c}_{SW} &\equiv c_{SW}u_0^3, \\ a\tilde{m} &\equiv am/u_0.\end{aligned}\tag{21}$$

We then obtain

$$\frac{1}{g_{\overline{MS}}^2(\mu)} = \frac{1}{g_\square^2(a)} + 2b_0 \ln a\mu - \tilde{t}_1^\square + (2b_1 \ln a\mu - \tilde{t}_2^\square) g_\square^2(a) + \dots\tag{22}$$

with

$$\begin{aligned}\tilde{t}_1^\square &= 0.1348680 - N_f \left(0.0066960 - 0.0050467 \tilde{c}_{SW} + 0.0298435 \tilde{c}_{SW}^2 \right. \\ &\quad \left. + a\tilde{m}(-0.0272837 + 0.0223503 \tilde{c}_{SW} - 0.0070667 \tilde{c}_{SW}^2) \right),\end{aligned}\tag{23}$$

$$\begin{aligned}\tilde{t}_2^\square &= 0.0217565 - N_f (0.000753 - 0.001053 \tilde{c}_{SW} + 0.000498 \tilde{c}_{SW}^2 \\ &\quad - 0.000474 \tilde{c}_{SW}^3 - 0.000104 \tilde{c}_{SW}^4).\end{aligned}\tag{24}$$

Changing t_1^\square to \tilde{t}_1^\square is simply a matter of replacing every c_{SW} by \tilde{c}_{SW} and every m by \tilde{m} , but the change in t_2^\square is not so simple, because the coefficients of the c_{SW} and c_{SW}^2 terms change. We see that tadpole improvement is successful in reducing the two-loop fermionic contribution: the largest coefficient in the fermionic part of t_2^\square was $0.01442\dots$, in \tilde{t}_2^\square it is $0.00105\dots$.

We are still free to choose the scale μ in eq. (22). A good value to help eq. (22) to converge rapidly is to choose μ so that the $O(g^0)$ term vanishes. Therefore we choose the scale so that

$$a\mu = \exp\left(\frac{\tilde{t}_1^\square}{2b_0}\right).\tag{25}$$

In the quenched case this gives $\mu = 2.63/a$, while for $N_f = 2$ dynamical fermions $\mu \approx 1.4/a$. Substituting this scale into eq. (22), we obtain the relationship

$$g_{\overline{MS}}^2(\mu) = g_\square^2(a) + \left(\tilde{t}_2^\square - \frac{b_1}{b_0}\tilde{t}_1^\square\right) g_\square^6(a) + O(g^8),\tag{26}$$

which agrees with [22] in the quenched case.

The calculation of $\Lambda_{\overline{MS}}$ proceeds in four steps. First we compute the average plaquette. From eq. (9) we then obtain g_\square . In the second step we use eq. (26) to calculate $g_{\overline{MS}}$ at the scale μ . Putting this value of $g_{\overline{MS}}$ into eq. (7) gives us $\mu/\Lambda_{\overline{MS}}$. Finally we use the conversion factor eq. (25) to turn this into a value for $a\Lambda_{\overline{MS}}$. To convert our results to a physical scale, we use the force parameter r_0 .

3 Results

$N_f = 0$

Let us begin with the quenched case. The plaquette values are taken from QCDSF's quenched simulations [27,28], except at $\beta = 6.57$ where the plaquette value is obtained by interpolation. The r_0 values are taken from [6,29]. In Fig. 2 we plot $\Lambda_{\overline{MS}} r_0$ against $(a/r_0)^2$. The corresponding numbers are given in Table 1. One expects discretization errors of $O(a^2)$. Indeed, the data points lie on a straight line, allowing a linear extrapolation to the continuum limit. This gives

$$\Lambda_{\overline{MS}}^{N_f=0} r_0 = 0.616(2)(25), \quad (27)$$

where the first error is purely statistical, while the second one is an estimate of the systematic error. The latter is derived by assuming that the higher-order contributions in eq. (26) are about 20% of the $O(g^6)$ term. Using $r_0 = 0.5$ fm, we find

$$\Lambda_{\overline{MS}}^{N_f=0} = 243(1)(10) \text{ MeV}. \quad (28)$$

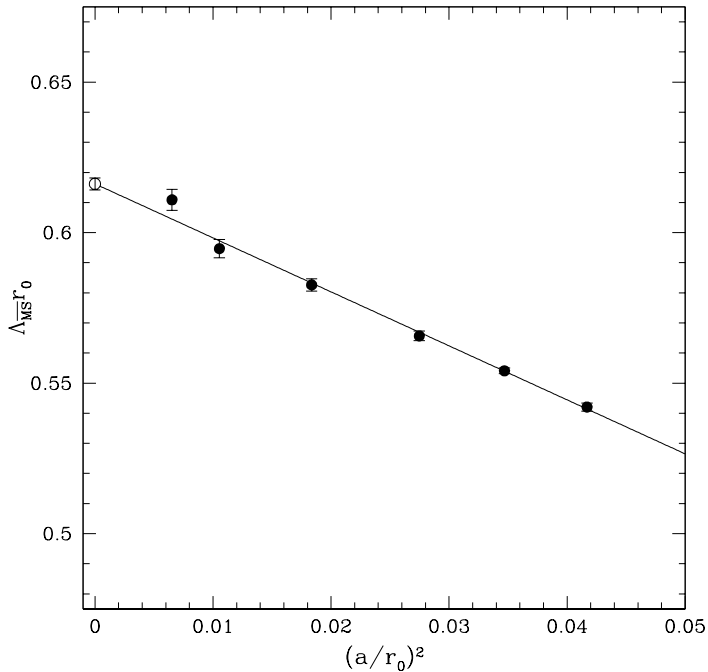


Fig. 2. The quenched scale parameter $\Lambda_{\overline{MS}} r_0$ against $(a/r_0)^2$ together with the continuum value (27). The coupling ranges from $\beta = 5.95$ to 6.57 . The line is a linear extrapolation to the continuum limit.

β	P	$(a/r_0)^2$	$\Lambda_{\overline{MS}}r_0$
5.95	0.588006(20)	0.04168(20)	0.5420(13)
6.00	0.593679(8)	0.03469(12)	0.5541(9)
6.07	0.601099(18)	0.02748(16)	0.5659(16)
6.20	0.613633(2)	0.01836(13)	0.5826(21)
6.40	0.630633(4)	0.01054(11)	0.5947(31)
6.57	0.6434(2)	0.00653(7)	0.6109(35)

Table 1

The quenched $\Lambda_{\overline{MS}}r_0$ values, together with $(a/r_0)^2$ and the plaquette P .

Our result agrees very well with the outcome of previous lattice calculations [9,15].

It should be noted that r_0 is a phenomenological quantity, though a very robust one, which introduces an additional systematic error. By comparing the results of various potential models we estimate the error to be less than 5%. Taking the ρ mass to set the scale gives [28] $r_0 = 0.52(2)$ fm, which is consistent with the value used in eq. (28).

$N_f = 2$

In the dynamical case we use combined results from the QCDSF and UKQCD collaborations [30,31]. The gauge field configurations were obtained using the standard Hybrid Monte Carlo algorithm with the non-perturbatively $O(a)$ improved action (2). Details of the extraction of r_0/a are given in [32]. For the quark mass m we take the Ward identity mass. We compute this mass in the same way [33] as in the quenched case [27], with the improvement coefficient c_A taken from tadpole improved perturbation theory. The relevant parameters and results are given in Table 2. The number of gauge field configurations varies from $O(500)$ on the $16^3 32$ lattices to $O(300)$ on the $24^3 48$ lattice.

As we are working at finite quark mass, we have to perform an extrapolation to the chiral limit. In Fig. 3 we show the parameter values of our simulations together with lines of constant r_0/a and m_π/m_ρ . This gives an impression of how far our simulations are from the chiral and continuum limits.

The value that interests us is $\Lambda_{\overline{MS}}$ at $m \rightarrow 0$ and $a \rightarrow 0$. Given the fact that our action has discretization errors of $O(a^2)$ only, at least as $m \rightarrow 0$, we expect the following small- a behavior: $\Lambda_{\overline{MS}}(a) = \Lambda_{\overline{MS}}(a=0)(1 + b_\Lambda am + O((a/r_0)^2) + O((am)^2))$, where $\Lambda_{\overline{MS}}(a=0)$ is not supposed to depend on m anymore. Similarly, we expect to find $r_0(a) = r_0(a=0)(1 + b_r am + O((a/r_0)^2) +$

β	κ_{sea}	V	c_{SW}	P	r_0/a	am	$\Lambda_{\overline{MS}} r_0$
5.20	0.1355	$16^3 32$	2.0171	0.536294(9)	5.041(40)	0.02364(16)	0.4744(38)
5.20	0.1350	$16^3 32$		0.533676(9)	4.754(40)	0.04586(19)	0.4593(39)
5.25	0.1352	$16^3 32$	1.9603	0.541135(24)	5.137(49)	0.04268(17)	0.4666(45)
5.26	0.1345	$16^3 32$	1.9497	0.539732(9)	4.708(52)	0.07196(20)	0.4348(48)
5.29	0.1355	$24^3 48$	1.9192	0.547081(26)	5.62(9)	0.03495(12)	0.4834(77)
5.29	0.1350	$16^3 32$		0.545520(29)	5.26(7)	0.05348(19)	0.4601(61)
5.29	0.1340	$16^3 32$		0.542410(9)	4.813(45)	0.09272(29)	0.4355(41)

Table 2

The dynamical $\Lambda_{\overline{MS}} r_0$ values, together with r_0/a , P and the quark masses. The improvement coefficient c_{SW} was taken from eq. (3).

$O((am)^2)$), with the difference that $r_0(a=0)$ may still depend on m : $r_0(a=0) = r_0(a=0, m=0)(1 + c_r m r_0 + O((m r_0)^2))$. Putting everything together,

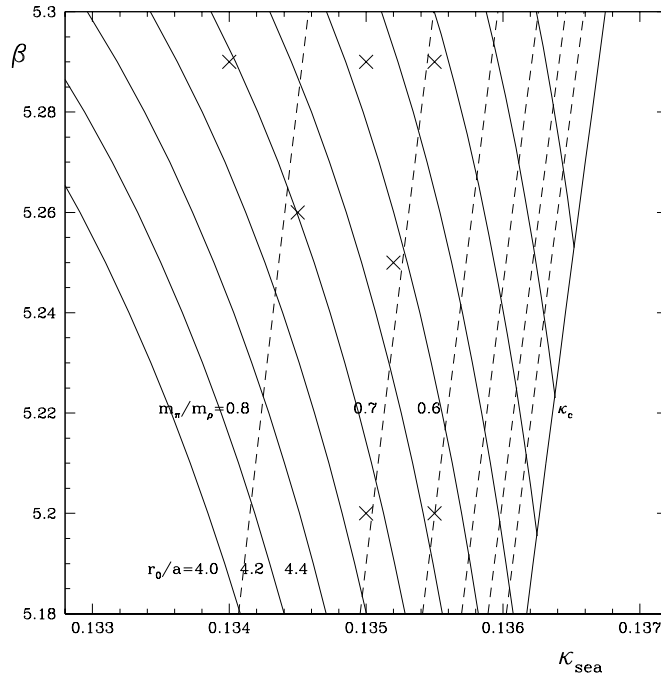


Fig. 3. Lines of constant r_0/a (full lines), from 4.0 (left) to 6.0 (right), and constant m_π/m_ρ (dashed lines), from 0.8 to 0.3, together with κ_c and the parameters (\times) of our simulations (up to now) in the $(\kappa_{\text{sea}}, \beta)$ plane. The curves are from a fit to the renormalization group and chiral perturbation theory, respectively.

we then arrive at the following parameterization of $\Lambda_{\overline{MS}} r_0$ for small a, m :

$$\Lambda_{\overline{MS}} r_0 = A(1 + Bam)(1 + Cmr_0) + D(a/r_0)^2, \quad (29)$$

where we have neglected terms of $O((mr_0)^2)$. Effectively $\Lambda_{\overline{MS}} r_0$ can be written as a function of mr_0 and a/r_0 .

We do not know c_A non-perturbatively. It turns out though that the final result is not affected by a small adjustment of c_A , for this changes all masses by a common factor, within the statistical errors, and hence amounts to a rescaling of the fit parameters B and C only.

Let us now turn to the fit and extrapolation of our data. In the fit we assume that $\Lambda_{\overline{MS}} r_0$, am and r_0/a are uncorrelated. We find that the ansatz (29) fits the data very well ($\chi^2 = 3.1$). The parameters B and C are strongly correlated though, indicating that it does not matter whether we are using am or mr_0 as the chiral extrapolation variable. Indeed, fixing $B = 0$ gives the same result for A and an almost identical value of χ^2 . To justify our ansatz (29), we subtract the mass dependence from the measured values of Λ to obtain $\Lambda_{\overline{MS}} r_0(m = 0) \equiv \Lambda_{\overline{MS}} r_0 - A(Bam + Cmr_0 + BCam mr_0)$. A plot of $\Lambda_{\overline{MS}} r_0(m = 0)$ against $(a/r_0)^2$ should then collapse all data points onto the single line $A + D(a/r_0)^2$. In the presence of significant higher-order terms not covered by our ansatz we would, on the other hand, expect to see the data deviate from that line. Similarly, a plot of $\Lambda_{\overline{MS}} r_0(a = 0) \equiv (\Lambda_{\overline{MS}} r_0 - D(a/r_0)^2)/(1 + Bam)$ against mr_0 should collapse the data onto the line $A(1 + Cmr_0)$. This is what we have plotted in Figs. 4 and 5. We see that it does indeed bring all data points onto one line. We also see that the deviations from the line are probably not statistically significant, so adding any extra term to the fit, like $(mr_0)^2$, the deviation from the line is just going to give a fit to the noise. In fact, we have experimented with higher-order polynomials in a and m . In all cases we found the same result in the chiral and continuum limit within the statistical error. Note that the slope of the line in Fig. 4 is very similar to the slope of the corresponding quenched line in Fig. 2.

In the chiral and continuum limit our fit gives

$$\Lambda_{\overline{MS}}^{N_f=2} r_0 = 0.549(39)(28). \quad (30)$$

The first error is purely statistical, while the second one is an estimate of the systematic error, where we again have assumed that the higher-order contributions in eq. (26) are about 20% of the $O(g^6)$ term. Using $r_0 = 0.5$ fm, this gives

$$\Lambda_{\overline{MS}}^{N_f=2} = 217(16)(11) \text{ MeV}. \quad (31)$$

A preliminary computation of the mass spectrum yields $r_0 = 0.50(7)$ fm, if we take the ρ mass to set the scale, in agreement with the phenomenological value used.

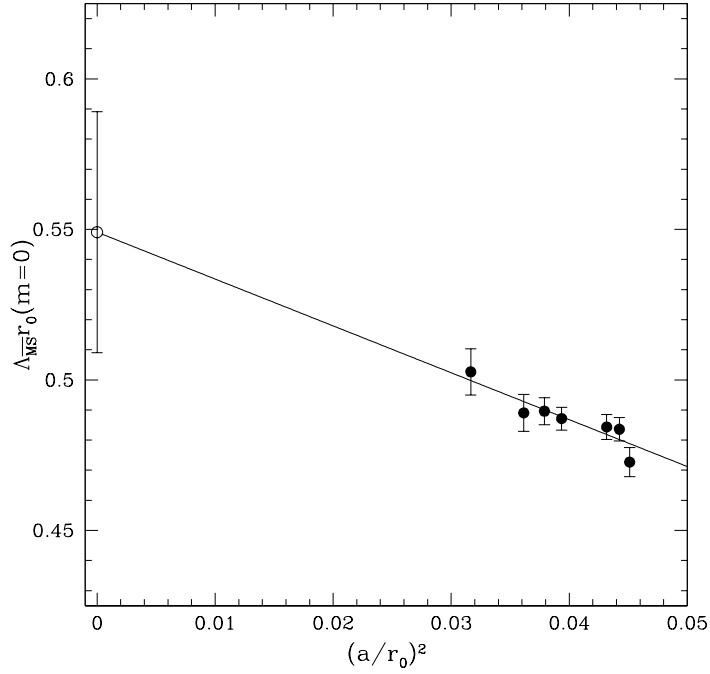


Fig. 4. The scale parameter $\Lambda_{\overline{MS}} r_0 (m = 0)$ against $(a/r_0)^2$ together with the fit (29) and the continuum result (30). The error of (30) shown is the statistical error only.

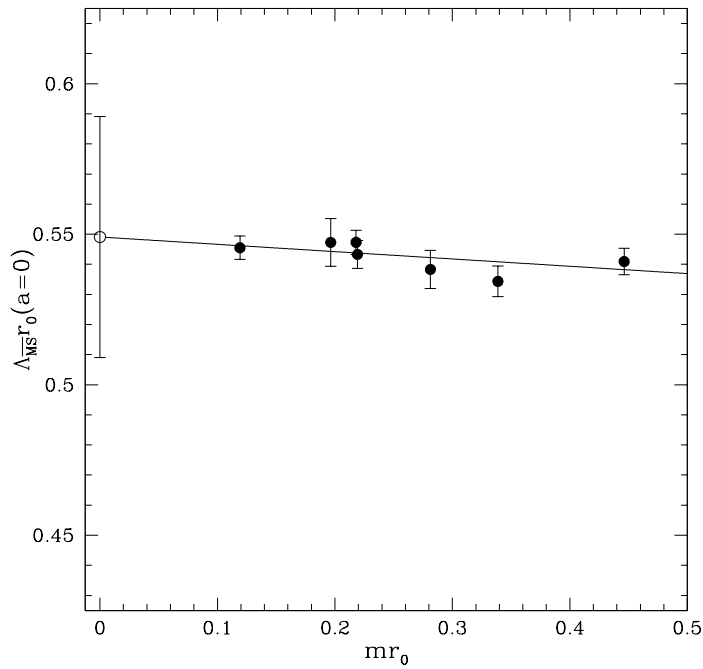


Fig. 5. The scale parameter $\Lambda_{\overline{MS}} r_0 (a = 0)$ against mr_0 together with the fit (29) and the continuum result (30).

Comparison with Phenomenology

How can our results be compared with the phenomenological numbers? A fit to the world data of α_s gives the average value at the Z mass [1] $\alpha_{\overline{MS}}^{N_f=5}(m_Z) = 0.118(2)$, which corresponds to $\Lambda_{\overline{MS}}^{N_f=5} = 208(25)$ MeV. The latter value refers to an idealized world of five massless quarks and thus cannot be compared immediately to our numbers. We may extrapolate $\Lambda_{\overline{MS}} r_0$ to three flavors (remember that r_0 is extracted from the phenomenological heavy quark potential) and then evolve the corresponding $\alpha_{\overline{MS}}$ to the Z mass, using the three-loop matching formulae [35]. We do this by extrapolating $\ln(\Lambda_{\overline{MS}} r_0)$ linearly in N_f to $N_f = 3$, ignoring the fact that the strange quark mass is already relatively heavy and therefore less effective. For $r_0 = 0.5$ fm this gives $\Lambda_{\overline{MS}}^{N_f=3} = 205(22)(20)$ MeV. (Allowing for a 5% uncertainty of the physical scale parameter r_0 would increase the systematic error only slightly to 22 MeV.) With the help of eq. (7) we now compute $\alpha_{\overline{MS}}^{N_f=3}$ at the scale $\mu = 1$ GeV and obtain $\alpha_{\overline{MS}}^{N_f=3}(1 \text{ GeV}) = 0.330(21)(19)$. Taking the charm and bottom thresholds to be at 1.5 GeV and 4.5 GeV, respectively, we then find $\alpha_{\overline{MS}}^{N_f=5}(m_Z) = 0.1076(20)(18)$, a number which is somewhat lower than the phenomenological value. If, on the other hand, we evolve the phenomenological value down to $N_f = 4$ and $N_f = 3$, we obtain $\Lambda_{\overline{MS}}^{N_f=4} = 292(31)$ MeV and $\Lambda_{\overline{MS}}^{N_f=3} = 342(32)$ MeV, respectively. A logarithmic extrapolation to $N_f = 2$, similar to our extrapolation of the lattice data but in reverse order, would give $\Lambda_{\overline{MS}}^{N_f=2} = 445(68)$ MeV.

In Fig. 6 we compare the Λ values obtained by the various methods. At energy scales below the charm mass threshold the physics should be determined by $\Lambda_{\overline{MS}}^{N_f=3}$. So one would expect that the lattice numbers extrapolate smoothly to the corresponding phenomenological value. We see, however, that this is not the case. The reason for this mismatch remains to be found.

4 Conclusions

Our quenched result agrees very well with results of other calculations using different methods. We find significant $O(a^2)$ corrections. For example at $\beta = 6.0$, corresponding to a lattice spacing $a \approx 0.1$ fm, they amount to $\approx 10\%$, which makes an extrapolation of the results to the continuum limit indispensable. In the dynamical case the data cover a much smaller range of a , which makes the extrapolation to the continuum limit less reliable. But it is reassuring to see that the continuum limit is approached at a similar rate as in the quenched case.

Our dynamical calculation is similar in spirit to previous unquenched com-

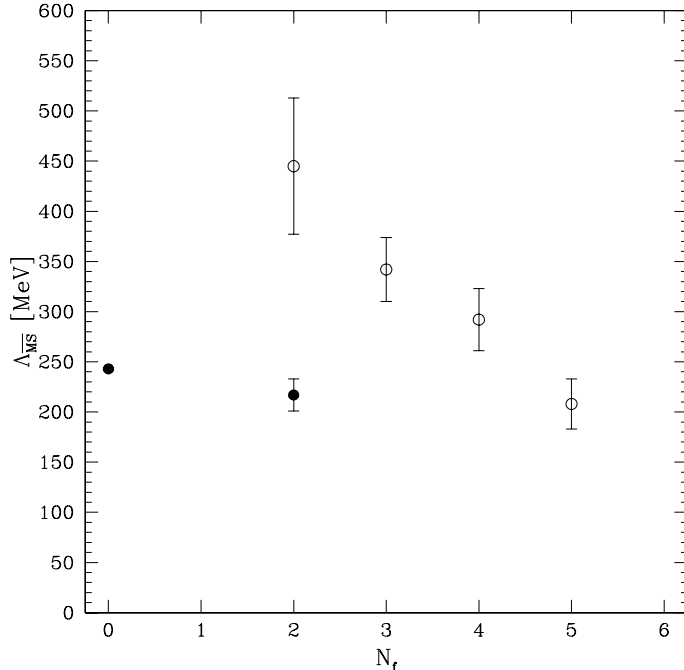


Fig. 6. The lattice (●) and phenomenological (○) scale parameters $\Lambda_{\overline{MS}}$ against N_f . The error bars of the lattice numbers correspond to the statistical errors.

putations of α_s [11–14] (albeit not exactly the same). The main differences are that we are using a non-perturbatively $O(a)$ improved fermion action, which reduces cut-off effects, the conversion to $g_{\overline{MS}}$ is done consistently in two-loop perturbation theory, and an extrapolation of Λ to the chiral and continuum limit is performed.

Appendix

We follow the argument in [34] calculating the relation between the Λ parameters from the potential. We require that the potential (or force) between two static charges should be the same, whether computed as a series in g^2 or $g_{\overline{MS}}^2$. All we have to do to calculate the fermionic piece of the relation is to compute the fermionic contribution to the gluon propagator.

In the scheme \mathcal{S} we have

$$\begin{aligned}
 V(\vec{r}) = & \int \frac{d^4q}{(2\pi)^4} 2\pi\delta(q_4) \frac{g_{\mathcal{S}}^2}{q^2} (1 - g_{\mathcal{S}}^2 G^{\mathcal{S}}(q^2)) \\
 & - g_{\mathcal{S}}^2 N_f \Pi^{\mathcal{S}}(q^2, m) + O(g_{\mathcal{S}}^4) e^{i\vec{q}\vec{r}},
 \end{aligned} \tag{32}$$

where $G^{\mathcal{S}}(q^2)$ is the one-loop gluon contribution to the potential, and $\Pi^{\mathcal{S}}$ is the one-loop quark vacuum polarization. If two schemes, \mathcal{S} and \mathcal{S}' , are to give

the same answer for $V(\vec{r})$, their couplings have to be related by

$$\frac{1}{g_S^2} = \frac{1}{g_{S'}^2} + \left(G^{S'}(q^2) - G^S(q^2) \right) + N_f \left(\Pi^{S'}(q^2, m) - \Pi^S(q^2, m) \right) + O(g^2). \quad (33)$$

To find the fermionic part of the conversion from g^2 to $g_{\overline{MS}}^2$, we have to calculate the vacuum polarization in both schemes and take the difference.

In the \overline{MS} scheme we find

$$\Pi^{\overline{MS}}(q^2, m) = -\frac{1}{24\pi^2} \left(\ln(q^2/\mu^2) - \frac{5}{3} + O(m^2/q^2) \right). \quad (34)$$

On the lattice we obtain

$$\begin{aligned} \Pi(q^2, m) = & -\frac{1}{24\pi^2} \left(\ln(a^2 q^2) - 3am(1 - c_{SW}) \ln(a^2 q^2) \right. \\ & - 3.25275141(5) + 1.19541770(1)c_{SW} - 7.06903716(4)c_{SW}^2 \\ & + am \left(6.46270704(30) - 5.29413266(6)c_{SW} \right. \\ & \left. \left. + 1.67389761(2)c_{SW}^2 \right) \right). \end{aligned} \quad (35)$$

We see that there is an unwanted $am \ln(a^2 q^2)$ term in eq. (35) unless $c_{SW} = 1 + O(g^2)$. Combining our calculation of Π with the calculation of the purely gluonic part in the literature [22], we get our final result for t_1 (for general N_c):

$$\begin{aligned} t_1 = & 0.16995600 N_c - \frac{1}{8N_c} \\ & - N_f \left(0.00669600 - 0.00504671 c_{SW} + 0.02984347 c_{SW}^2 \right. \\ & \left. + am \left(-0.02728371 + 0.02235032 c_{SW} - 0.00706672 c_{SW}^2 \right) \right). \end{aligned} \quad (36)$$

The am term in eq. (36) means that in dynamical QCD the contours of constant $g_{\overline{MS}}^2(1/a)$ will be slanted when plotted in a (am, β) plane. As one expects the contours of constant r_0/a to roughly follow contours of constant $g_{\overline{MS}}^2(1/a)$, this term gives a possible explanation of the appearance of the sloped lines in Fig. 3.

Acknowledgement

We thank H. Panagopoulos for communicating the three-loop β function for improved Wilson fermions to us prior to publication. The numerical calculations have been performed on the Hitachi SR8000 at LRZ (Munich), on the Cray T3E at EPCC (Edinburgh), NIC (Jülich) and ZIB (Berlin) as well as on the APE/Quadrics at DESY (Zeuthen). We thank all institutions for

their support. This work has been supported in part by the European Community's Human Potential Program under contract HPRN-CT-2000-00145, Hadrons/Lattice QCD. MG and PELR acknowledge financial support from DFG.

References

- [1] Particle Data Group, Eur. Phys. J. C15 (2000) 1.
- [2] P. Weisz, Nucl. Phys. B (Proc. Suppl.) 47 (1996) 71.
- [3] J. Shigemitsu, Nucl. Phys. B (Proc. Suppl.) 53 (1997) 16.
- [4] S.P. Booth, D.S. Henty, A. Hulsebos, A.C. Irving, C. Michael and P.W. Stephenson, Phys. Lett. B294 (1992) 385.
- [5] G.S. Bali and K. Schilling, Phys. Rev. D47 (1993) 661.
- [6] R.G. Edwards, U.M. Heller and T.R. Klassen, Nucl. Phys. B517 (1998) 377.
- [7] J.I. Skullerud, Nucl. Phys. B (Proc. Suppl.) 63 (1998) 242.
- [8] B. Allés, D.S. Henty, H. Panagopoulos, C. Parrinello, C. Pittori and D.G. Richards, Nucl. Phys. B502 (1997) 325.
- [9] P. Boucaud, G. Burgio, F. DiRenzo, J.P. Leroy, J. Micheli, C. Parrinello, O. Pène, C. Pittori, J. Rodriguez-Quintero, C. Roiesnel and K. Sharkey, JHEP 0004 (2000) 006.
- [10] A.X. El-Khadra, G. Hockney, A.S. Kronfeld and P.B. Mackenzie, Phys. Rev. Lett. 69 (1992) 729.
- [11] S. Aoki, M. Fukugita, S. Hashimoto, N. Ishizuka, H. Mino, M. Okawa, T. Onogi and A. Ukawa, Phys. Rev. Lett. 74 (1995) 22.
- [12] M. Wingate, T. DeGrand, S. Collins and U.M. Heller, Phys. Rev. D52 (1995) 307.
- [13] C.T.H. Davies, K. Hornbostel, G.P. Lepage, P. McCallum, J. Shigemitsu and J. Sloan, Phys. Rev. D56 (1997) 2755.
- [14] A. Spitz, H. Hoerber, N. Eicker, S. Güsken, T. Lippert, K. Schilling, T. Struckmann, P. Ueberholz and J. Viehoff, Phys. Rev. D60 (1999) 074502.
- [15] S. Capitani, M. Lüscher, R. Sommer and H. Wittig, Nucl. Phys. B544 (1999) 669.
- [16] R. Sommer, Nucl. Phys. B411 (1994) 839.
- [17] B. Sheikholeslami and R. Wohlert, Nucl. Phys. B259 (1985) 572.
- [18] K. Jansen and R. Sommer, Nucl. Phys. B530 (1998) 185.

- [19] T. van Ritbergen, J.A.M. Vermaseren and S.A. Larin, Phys. Lett. B400 (1997) 379; J.A.M. Vermaseren, S.A. Larin and T. van Ritbergen, Phys. Lett. B405 (1997) 327.
- [20] G. Parisi, in *High Energy Physics - 1980*, Proceedings of the XXth International Conference, Madison, eds. L Durand and L.G. Pondrom (American Institute of Physics, New York, 1981); G.P. Lepage and P.B. Mackenzie, Phys. Rev. D48 (1993) 2250.
- [21] F. DiRenzo, G. Marchesini and E. Onofri, Nucl. Phys. B457 (1995) 202; F. DiRenzo and L. Scorzato, [hep-lat/0011067](#).
- [22] M. Lüscher and P. Weisz, Phys. Lett. B349 (1995) 165; M. Lüscher, [hep-lat/9802029](#).
- [23] B. Allés, A. Feo and H. Panagopoulos, Phys. Lett. B426 (1998) 361.
- [24] S. Sint, private notes (1996), quoted in A. Bode, P. Weisz and U. Wolff, Nucl. Phys. B576 (2000) 517.
- [25] L. Marcantonio, P. Boyle, C.T.H. Davies, J. Hein and J. Shigemitsu, Nucl. Phys. B (Proc. Suppl.) 94 (2001) 363.
- [26] A. Bode and H. Panagopoulos, to be published.
- [27] M. Göckeler, R. Horsley, H. Perlt, P.E.L. Rakow, G. Schierholz, A. Schiller and P. Stephenson, Phys. Rev. D57 (1998) 5562; M. Göckeler, R. Horsley, D. Pleiter, P.E.L. Rakow, G. Schierholz and P. Stephenson, Nucl. Phys. B (Proc. Suppl.) 83 (2000) 203.
- [28] D. Pleiter, Thesis, Berlin (2000); QCDSF *Collaboration*, in preparation.
- [29] M. Guagnelli, R. Sommer and H. Wittig, Nucl. Phys. B535 (1998) 389.
- [30] H. Stüben, Nucl. Phys. B (Proc. Suppl.) 94 (2001) 273.
- [31] A.C. Irving, Nucl. Phys. B (Proc. Suppl.) 94 (2001) 242.
- [32] C.R. Allton, S.P. Booth, K.C. Bowler, J. Garden, A. Hart, D. Hepburn, A.C. Irving, B. Joo, R.D. Kenway, C.M. Maynard, C. McNeile, C. Michael, S.M. Pickles, J.C. Sexton, K.J. Sharkey, Z. Sroczynski, M. Talevi, M. Teper and H. Wittig, [hep-lat/0107021](#).
- [33] D. Pleiter, Nucl. Phys. B (Proc. Suppl.) 94 (2001) 265.
- [34] I. Montvay and G. Münster, *Quantum Fields on a Lattice* (Cambridge Univ. Press, Cambridge, 1994).
- [35] K.G. Chetyrkin, J.H. Kühn and M. Steinhauser, Comput. Phys. Commun. 133 (2000) 43.